Introduction

The complete description of the morphology and synaptic connectivity of all 302 neurons in the nematode *Caenorhabditis elegans* raised the prospect of the first comprehensive understanding of the neuronal basis of an animal's entire behavioral repertoire. The advent of new electrophysiological and functional imaging techniques for *C. elegans* neurons has made this project more realistic than before. Further progress would be accelerated, however, by prior knowledge of the sensorimotor transformations underlying the behaviors of *C. elegans*, together with knowledge of how these transformations could be implemented with *C. elegans*-like neuronal elements. Here, we used a computer algorithm to search for patterns of synaptic connectivity sufficient to compute the sensorimotor transformation underlying chemotaxis. Common patterns of connectivity between the model and biological network suggest new functions for previously identified connections in the *C. elegans* nervous system.

Assumptions

1. Primary chemosensory neurons in *C. elegans* report attractant concentration at a single point in space.
2. Chemosensory interneurons converge on a network of locomotory command neurons to regulate turning probability.
3. The sensorimotor transformation in *C. elegans* is computed mainly at the network level, not at the cellular level.

Network

Neurons were modeled by the equation:

$$\tau_i \frac{dA_i(t)}{dt} = -A_i(t) + \sigma(I_i), \quad \texttt{with} \quad I_i = \sum_j (w_{ji} A_j(t)) + b_i \qquad (1)$$

$A_i(t)$ is the activation level of neuron i in the network, $\sigma(I_i)$ is the logistic function $1/(1+e^{-I_i})$, w_{ji} is the synaptic strength from neuron j to neuron i, and b_i is static bias. The time constant τ_i determines how rapidly the activation approaches its steady-state value for constant I_i.

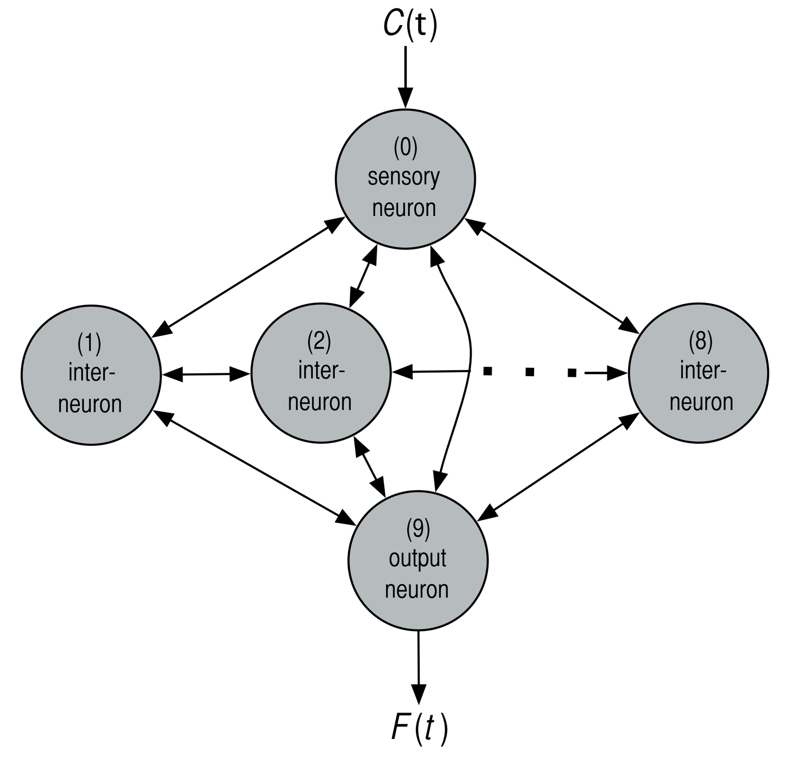

Figure 1: Model chemosensory network. Model neurons were passive, isopotential nodes. The network contained one sensory neuron, one output neuron, and eight interneurons. Input to the sensory neuron was the time course of chemoattractant concentration *C*(*t*). The activation of the output neuron was mapped to turning probability by the function *F*(*t*) given in Equation 2. The network was fully connected with self-connections (not shown).

The activity level of the output neuron (i = 9) determined the behavioral state of the model, i.e. turning probability, according to the piecewise function:

$$F(t) = \begin{cases} P_{high} & A_9(t) \geq T_2 \\ P_{rest} & T_1 < A_9(t) < T_2 \\ P_{low} & A_9(t) \leq T_1 \end{cases} \qquad (2)$$

T_1 and T_2 are arbitrary thresholds and the three P values represent the indicated levels of turning probability.

Optimization

The chemosensory network model was optimized to compute an idealized version of the true sensorimotor transformation linking *C*(*t*) to turning probability. To construct the idealized transformation, we mapped the instantaneous derivative of *C*(*t*) to desired turning probability *G*(*t*) as follows:

$$G(t) = \begin{cases} P_{high} & dC(t)/dt \leq -U \\ P_{rest} & -U < dC(t)/dt < +U \\ P_{low} & dC(t)/dt \geq +U \end{cases} \qquad (3)$$

U is a threshold derived from previous behavioral observations. The goal of the optimization was to make the network's turning probability *F*(*t*) equal to the desired turning probability *G*(*t*) at all *t*. Optimization was carried out by adjusting three parameters: synaptich strengths, time constants, and biases (equation 1).

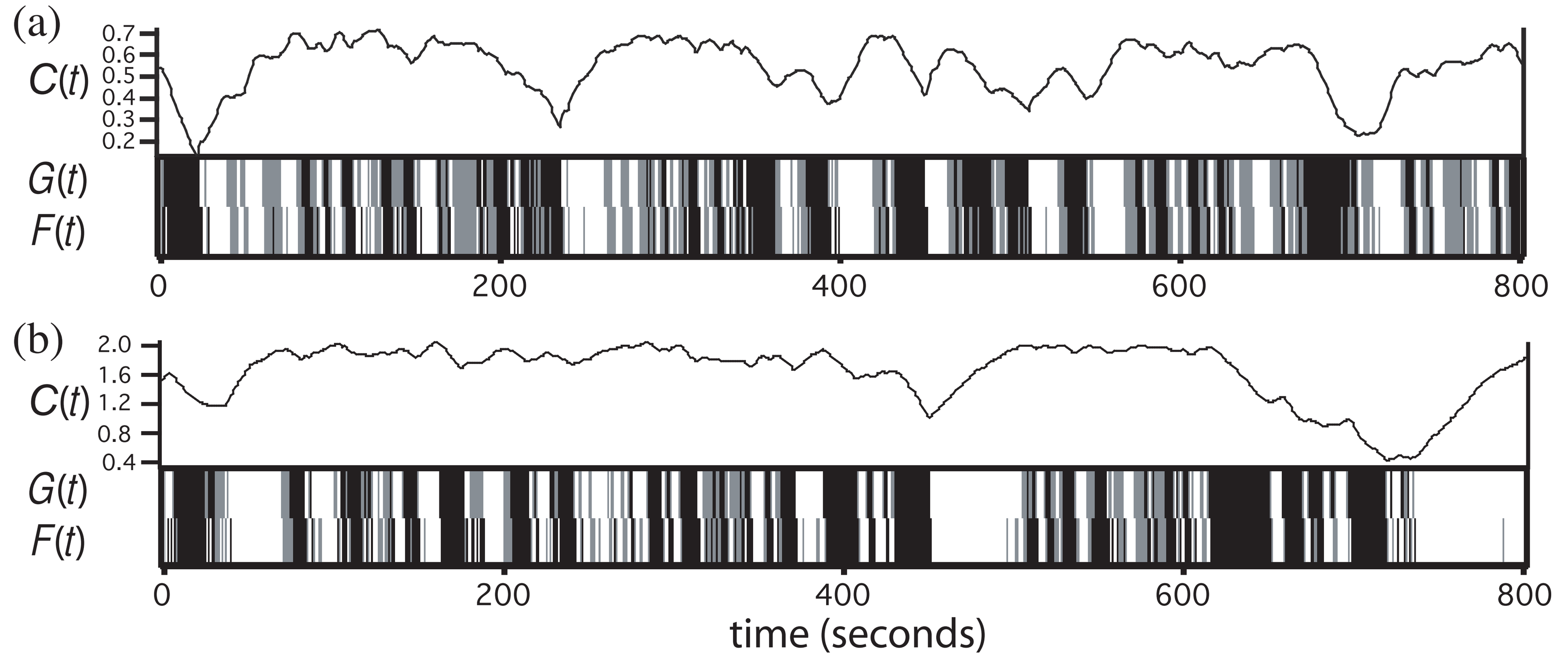

Figure 2: Network performance after optimization. In each panel, the upper trace represents *G*(*t*), the desired turning probability in response to a particular *C*(*t*) time course, whereas the lower trace represents *F*(*t*), the resulting network turning probability. Shading signifies turning probability (black = P_{high}, grey = P_{rest}, white = P_{low}). (a) Performance of a typical network after optimization. (b) Performance of the network when stimulated by a different *C*(*t*) time course. Network turning probability is delayed relative to desired turning probability because of the time required for sensory input to affect behavioral state.

Results

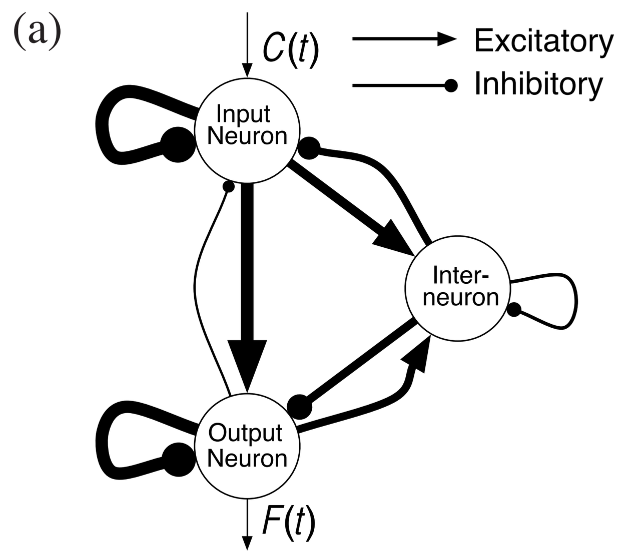

(b)

Feature	Figure	Function
direct excitatory delayed inhibitory	slow	differentiation
self-connection		hypothesis: regulation of response latency
inhibitory recurrent connection		

Figure 3: Connectivity and common features of single-interneuron networks. (a) Average sign and strength of connections. Line thickness is proportional to connection strength. In other single-interneuron networks, the sign of the connections to and from the interneuron were reversed (not shown). (b) The three common features of single-interneuron networks.

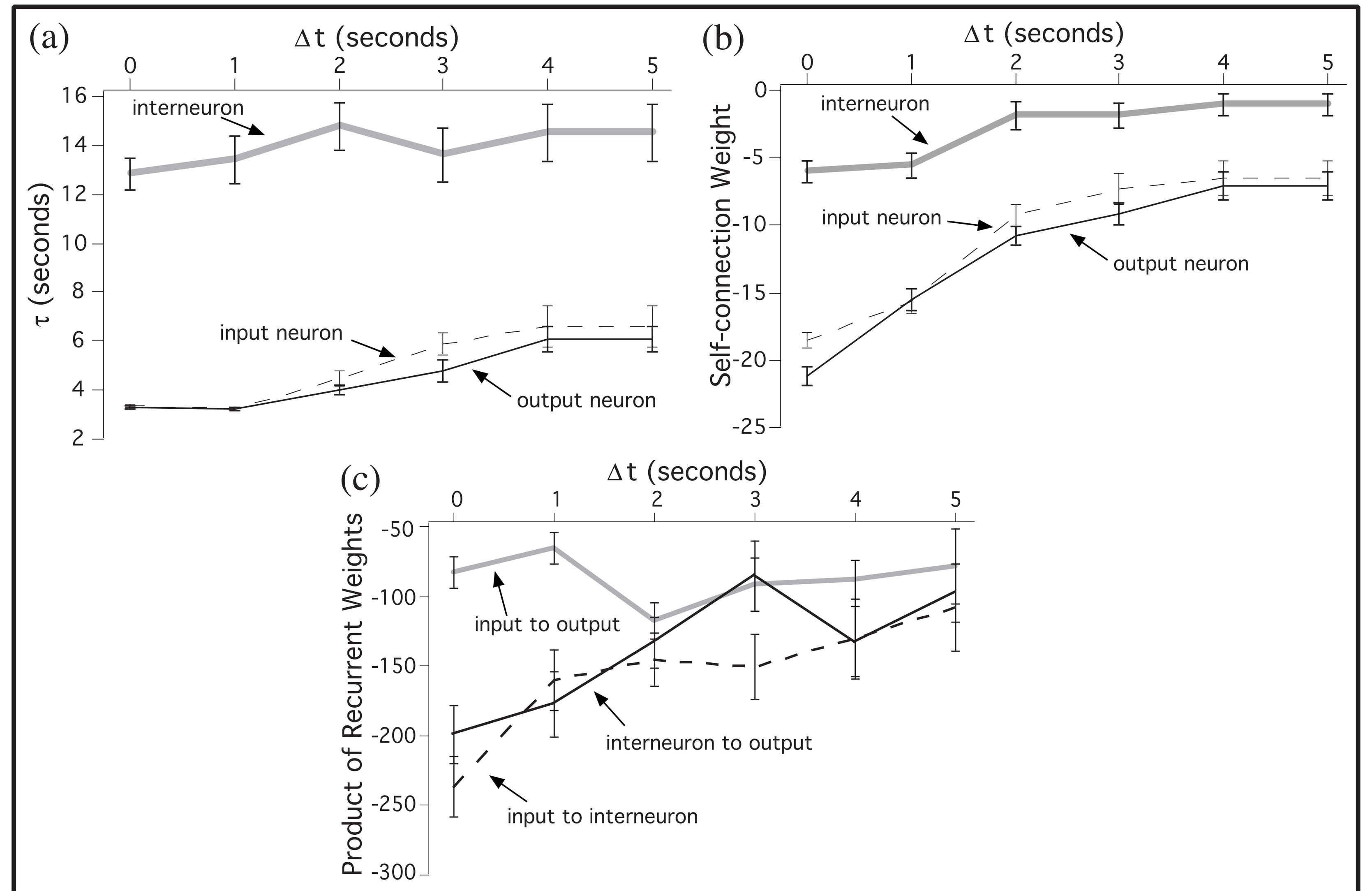

Figure 4: The effect on connectivity of introducing time delays between input *C*(*t*) and output *G*(*t*) during optimization. (a) The effect on the neuronal time constant. (b) The effect on self-connections. (c) The effect on recurrent connections. Recurrent connection strength was quantified by taking the product of the weights along each of the three recurrent loops in Figure 3(a). These results suggest that the function of the inhibitory feedback provided by self-connections and recurrent connections is to regulate response latency.

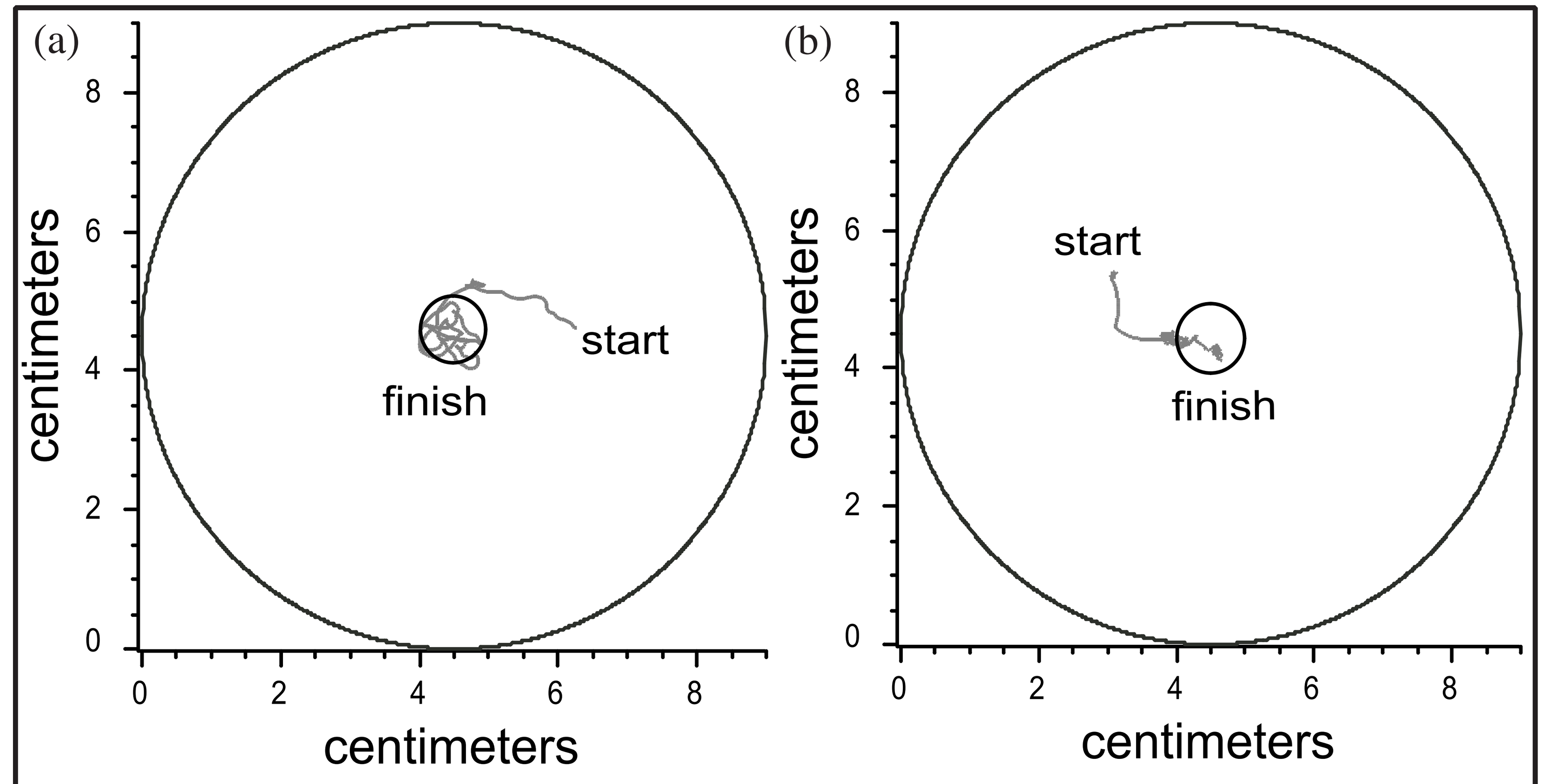

Figure 5: A sample track of a live *C. elegans* chemotaxing towards an attractant (NH4Cl) (a) compared with a simulated track (b). The simulated worm uses a three-neuron neural network optimized to produce behavior from chemical stimulus. The success rate to the center is similar for both the experimental worm (a): 93.6%, N=31 and the simulated worm (b): 94.4%, N=1000. Successfull chemotaxis is defined as if a worm is able to reach within a 0.5 cm radius from the center. Average starting positions is defined as 1.1 cm from the center.

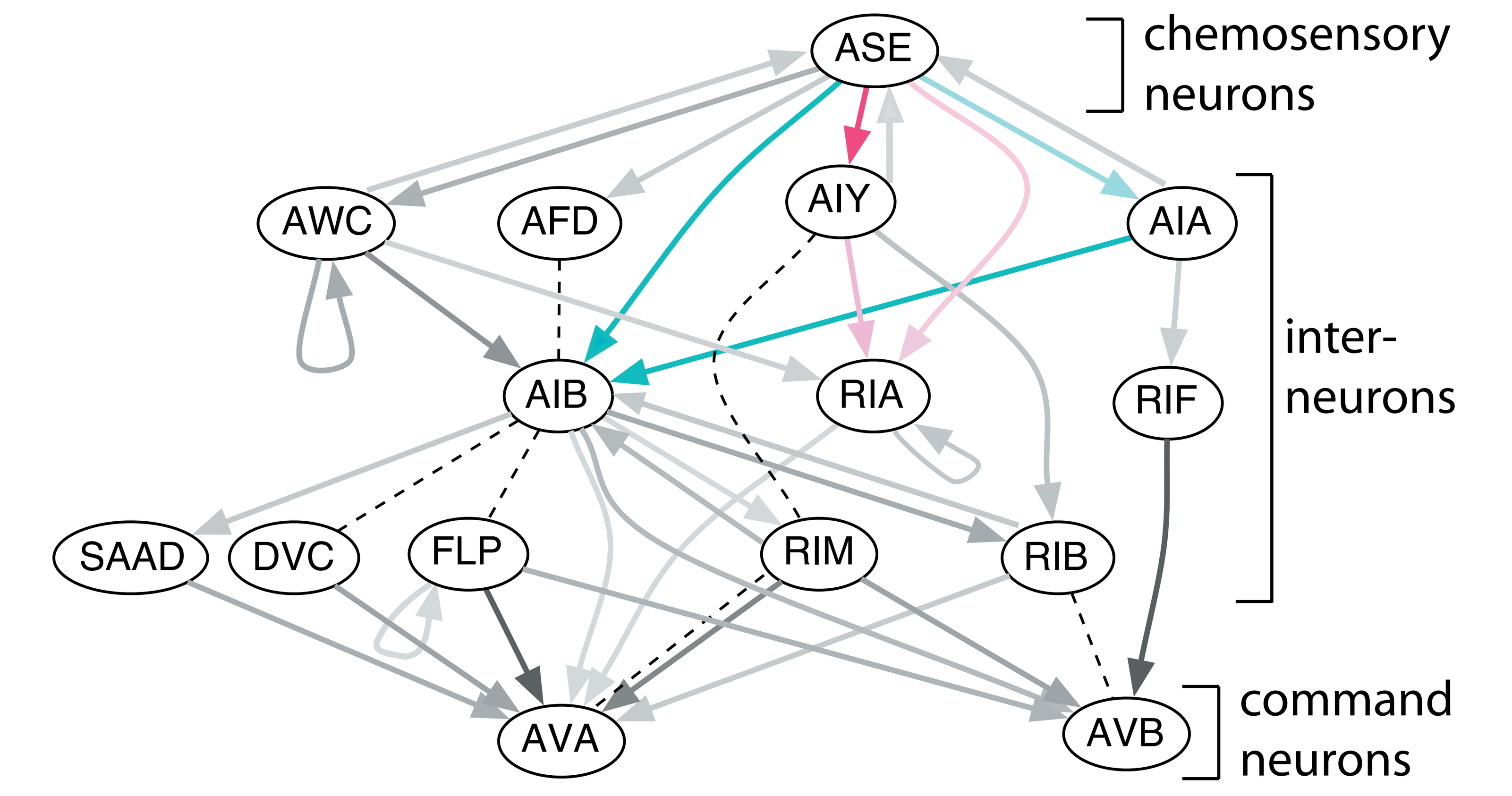

Figure 6: The network of chemosensory interneurons in the real animal. Shown are the interneurons interposed between the chemosensory neuron ASE and the two locomotory command neurons AVA and AVB. The diagram is restricted to synaptic pathways of less than three connections. Arrows represent chemical synapses, where the darkness of the line is a proportional to the number of connections. Dashed lines represent gap junctions. Connectivity is inferred from the anatomical reconstructions in White et. al. 1986. Two possible three-neuron connections are shown in red and blue, going through the interneurons AIY and AIA, respectively.

Conclusion

- Common patterns of connectivity between the model and biological networks suggest new functions for previously identified connections in the *C. elegans* nervous system.
- It should be possible to test these functions through physiological recordings and neuronal ablations.